Scheme I

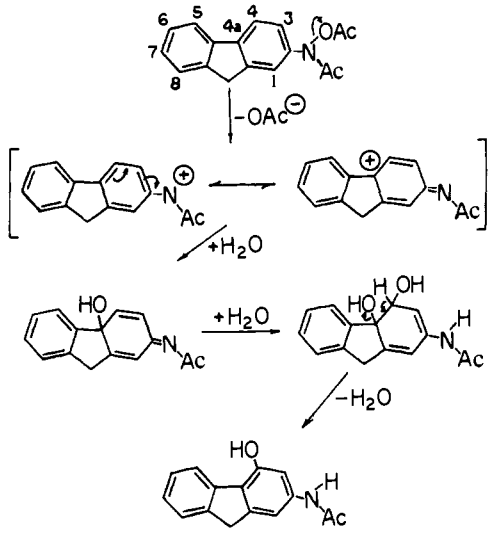

with 25% ethyl acetate in benzene. Although both TLC and the column procedure show clearly a product which appears to be at least half of the detectable material, only ~10% of the starting material can be isolated in this fraction as pure solid. Other products were isolated in still smaller quantities as expected. However, a high-melting compound which was almost insoluble in ether or ethyl acetate, and did not migrate on TLC, may account for the remainder of the starting material. Even the dilution used here is a significantly higher concentration than that used by Gutmann et al., and this higher concentration may result in extensive formation of dimers or higher polymers which would reduce the yield of **2** below that found by Gutmann et al. A mass spectrum showed that **2** was a hydroxylated acetamidofluorene, an observation confirmed by the infrared spectrum. NMR spectrometry suggested that the aromatic ring not carrying the nitrogen was not further substituted. Ultraviolet spectra in neutral and basic ethanol confirmed that the substance was a phenol, but the UV spectrum was clearly different from those of both 1- and 3-hydroxy-2-acetamidofluorene (which also are much less polar on adsorption chromatography). Thus, unlikely as it seemed, the only rational conclusion was that **2** is 4-hydroxy-2-acetamidofluorene. This conclusion was initially confirmed by comparison of the UV spectrum with that of 4-hydroxy-2-formylaminofluorene.[3] Further confirmation was obtained by comparison of the infrared spectrum of the acetate of **2** with the spectrum of authentic 4-acetoxy-2-acetamidofluorene, generously provided by Dr. T. L. Fletcher.

This conversion is a most unusual reaction, for all previously known reactions of **1** take place on the nitrogen atom,[4] or on positions 3 and 1.[5] This past experience was confirmed by my being able to prepare 3-chloro-2-acetamidofluorene[6] in 40% yield simply by dissolving **1** (500 mg in 50 mL of acetone) in 1 L of 1 M NH_4Cl heated to 50 °C, extracting the warm mixture 2 h later, and recrystallizing the residue from the extract. I suggest that **2** arises from initial hydroxylation of position 4a of the intermediate *N*-acetyl-*N*-fluorenylnitrenium ion, followed by further hydration of the ensuing quinone imide methide,[7] and dehydration of the resulting diol (Scheme I). This mechanism is suggested by an examination of the coefficients of the lowest unoccupied molecular orbital of the nitrenium ion, which shows position 4a to be more reactive than any other aromatic carbon. An explanation of why other nucleophiles do not attack this carbon will have to await molecular orbital calculations which specifically address the interaction between the delocalized nitrenium ion and sulfur, nitrogen, or chloride. Steric accessibility is not a factor in attack by chloride, according to space-filling models.

This study points out again the tenuous nature of identifications based only on chromatographic properties, and renders pointless much of the discussion offered previously by Gutmann et al. regarding the possible role of *N*-acetoxyacetamidofluorenes in mammary gland carcinogenesis by the corresponding hydroxamic acids. On the other hand, this finding may have considerable significance for further studies on the mechanism of carcinogenesis by 2-acetamidofluorene and other aromatic amines. The sulfate ester of *N*-hydroxy-2-acetamidofluorene is believed to be the ultimate reactive form in the carcinogenic action of 2-acetamidofluorene toward the liver of the male rat.[5b] In the absence of other nucleophiles, it would be expected to react with water similarly to **1**; yet 4-hydroxy-2-acetamidofluorene has not been observed among the urinary metabolites of 2-acetamidofluorene or its *N*-hydroxy derivative.[8] Hence, it appears that bound forms of 2-acetamidofluorene in the rat represent virtually all of the sulfate ester. Therefore, the level of binding to macromolecules and other intracellular nucleophiles is a direct measure of the amount of active intermediates formed, rather than an unknown proportion of some larger amount. It is thus possible to estimate what proportion of the total dose of 2-acetamidofluorene is converted to reactive metabolite. It is also possible that minute quantities of 4-hydroxy-2-acetamidofluorene were overlooked in previous metabolic studies. This point may deserve reinvestigation.

Acknowledgments. This work was supported by Grant CA 18632 from the National Cancer Institute of the U.S. Public Health Service. I thank R. Hodson and S. R. Fisk for technical assistance. The NMR spectrum was provided by Dave Wilbur, Frederick Cancer Research Center; the mass spectrum was obtained by Elliott Hills, Michigan Cancer Foundation.

References and Notes

(1) H. R. Gutmann, D. Malejka-Giganti, and R. McIver, *J. Chromatogr.*, **115**, 71–78 (1975).
(2) J. D. Scribner, J. A. Miller, and E. C. Miller, *Cancer Res.*, **30**, 1570–1579 (1970).
(3) H.-L. Pan and T. L. Fletcher, *J. Org. Chem.*, **25**, 1106–1109 (1960).
(4) E. Kriek, J. A. Miller, U. Juhl, and E. C. Miller, *Biochemistry*, **6**, 177–182 (1967).
(5) (a) P. D. Lotlikar, J. D. Scribner, J. A. Miller, and E. C. Miller, *Life Sci.*, **5**, 1263–1269 (1966); (b) J. R. DeBaun, E. C. Miller, and J. A. Miller, *Cancer Res.*, **30**, 577–595 (1970); (c) J. G. Westra, E. Kriek, and H. Hittenhausen, *Chem.-Biol. Interact.*, **15**, 149–164 (1976).
(6) F. Bell and J. A. Gibson, *J. Chem. Soc. (London)*, 3560–3562 (1955).
(7) J. D. Scribner, *J. Org. Chem.*, **41**, 3820–3824 (1976).
(8) (a) J. A. Weisburger, E. K. Weisburger, H. P. Morris, and H. A. Sober, *J. Natl. Cancer Inst.*, **17**, 363–374 (1956); (b) E. K. Weisburger and J. H. Weisburger, *Adv. Cancer Res.*, **5**, 331–431 (1958); (c) J. H. Weisburger, E. K. Weisburger, P. H. Grantham, and H. P. Morris, *J. Biol. Chem.*, **234**, 2138–2140 (1959); (d) J. A. Miller, J. W. Cramer, and E. C. Miller, *Cancer Res.*, **20**, 950–962 (1960).
(9) This is part 5 in the series "*N*-Arylnitrenium Ions in Aromatic Amine Carcinogenesis".

John D. Scribner[9]
Pacific Northwest Research Foundation
Seattle, Washington 98104
Received July 8, 1977

Synthesis and Crystal Structure of $H_4Ru_4(CO)_{10}(Ph_2PCH_2CH_2PPh_2)$. Evidence for an Edge–Terminal-Edge Hydride Scrambling Pathway

Sir:

The contrasting hydride ligand positions adopted in highly symmetrical H_4M_4 cluster compounds—edge bridging in D_{2d} $H_4Ru_4(CO)_{12}$[1] vs. face bridging in T_d $H_4Re_4(CO)_{12}$[2,3] and $H_4CO_4(\eta^5\text{-}C_5H_5)_4$[4]—pose the question whether interconversion between the two arrangements could provide a mechanism for hydride scrambling over the M_4 framework. Hydride

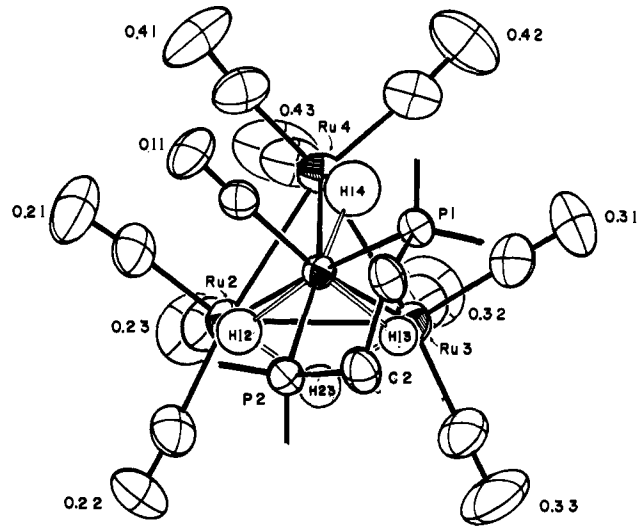

Figure 1. The $H_4Ru_4(CO)_{10}(Ph_2PCH_2CH_2PPh_2)$ molecule, with phenyl groups omitted, projected onto its Ru(2)–Ru(3)–Ru(4) plane. Ru(1) is unlabeled and is shaded in the center of the figure.

mobility has been established for the derivatives $H_4Ru_4(CO)_{12-x}[P(OMe)_3]_x$ (x = 1–3)[1,5] and $[H_3Ru_4(CO)_{12}^-]$,[6] but the NMR data do not delineate the exchange mechanism, i.e., do not show whether an edge–face-edge pathway obtains. We have prepared and structurally characterized a new derivative, $H_4Ru_4(CO)_{10}(Ph_2PCH_2CH_2PPh_2)$ (**1**). Contrary to expectations based on observed structures,[7] this compound displays NMR spectra consistent with an edge–terminal-edge hydride scrambling pathway.

Compound **1** was prepared from $H_4Ru_4(CO)_{12}$ and $Ph_2PCH_2CH_2PPh_2$ in refluxing cyclohexane, separated by column chromatography from other, unidentified products, and isolated as red-orange crystals.[9] A single-crystal x-ray diffraction study has accurately located all atoms, including the four μ_2-hydride ligands.[10] The principal features of the structure are illustrated in Figure 1. The diphosphine ligand chelates to Ru(1). Bond distances within the five-membered ring are as follows: Ru(1)–P(1) = 2.303 (2), P(1)–C(1) = 1.846 (6), C(1)–C(2) = 1.529 (8), C(2)–P(2) = 1.834 (6), and P(2)–Ru(1) = 2.321 (2) Å. The μ_2-hydride bridged Ru···Ru vectors are Ru(1)–Ru(2) = 2.998 (1), Ru(1)–Ru(3) = 3.006 (1), Ru(1)–Ru(4) = 2.946 (1), and Ru(2)–Ru(3) = 2.931 (1) Å. These are expanded by some 0.18 Å (average) from the nonbridged ruthenium–ruthenium bonds Ru(2)–Ru(4) = 2.796 (1) and Ru(3)–Ru(4) = 2.785 (1) Å. The individual Ru–H–Ru systems appear to be symmetric, with interatomic distances and angles as follows: Ru(1)–H(12) = 1.73 (5) Å, Ru(2)–H(12) = 1.80 (4) Å, ∠Ru(1)–H(12)–Ru(2) = 116 (3)°; Ru(1)–H(13) = 1.77 (4) Å, Ru(3)–H(13) = 1.80 (4) Å, ∠Ru(1)–H(13)–Ru(3) = 115 (2)°; Ru(1)–H(14) = 1.64 (6) Å, Ru(4)–H(14) = 1.76 (5) Å, ∠Ru(1)–H(4)–Ru(4) = 120 (3)°; and Ru(2)–H(23) = 1.81 (4) Å, Ru(3)–H(23) = 1.78 (5) Å, ∠Ru(2)–H(23)–Ru(3) = 110 (2)°. Although the $H_4Ru_4(CO)_{10}(Ph_2PCH_2CH_2PPh_2)$ molecule overall obeys the EAN rule (60 valence electrons), individual ruthenium atoms do not. The hydride ligand arrangement, with three hydrides bound to Ru(1) but only one to Ru(4), contrasts with the arrangement of two hydrides attached to each ruthenium atom deduced for $H_4Ru_4(CO)_{12}$,[1] $H_4Ru_4(CO)_{11}P(OMe)_3$,[3] and $H_4Ru_4(CO)_{10}(PPh_3)_2$.[11]

The slow-exchange hydride NMR spectrum of **1** displays P–H coupling patterns[12] that are readily interpreted in terms of the solid-state structure. A triplet (A) at τ 29.2 is assigned to the hydride H(13) oriented cis to both phosphorus atoms and a singlet (D) at τ 26.5 to the remote hydride H(23). Two double doublets at τ 26.1 (C) and 24.8 (B) result from the remaining hydrides (H(12), H(14)), each of which is cis (smaller coupling) to one phosphorus atom and trans (larger coupling) to the other. Between −50 and 25 °C the B, C, and D resonances collapse and coalesce to a broad singlet, while the A triplet remains unchanged. Above room temperature both of these signals broaden considerably; their presumptive coalescence could not be observed owing to sample decomposition.

Figure 2 shows intermediate exchange spectra for the B, C, and D signals. The significant feature is that the inner two lines of the C multiplet broaden much more slowly than the other lines. This implies that the initial dynamic process does not

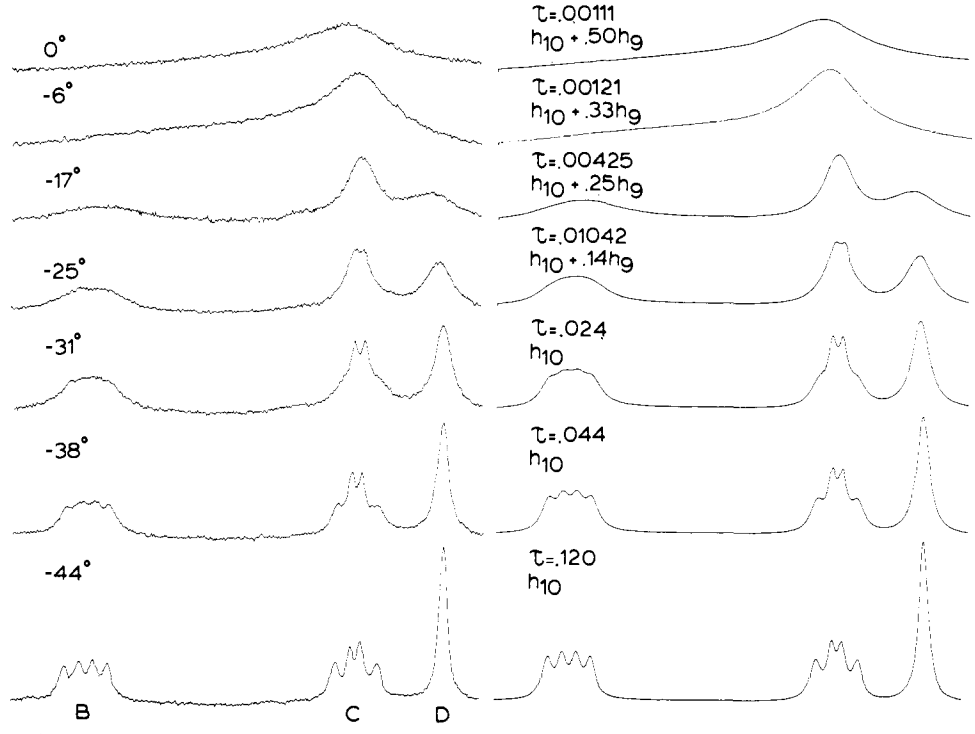

Figure 2. Partial hydride NMR (220 MHz) spectra for **1** in the intermediate exchange region. Not shown is the triplet resonance (A) at τ 29.2, which remains unchanged over this temperature range.

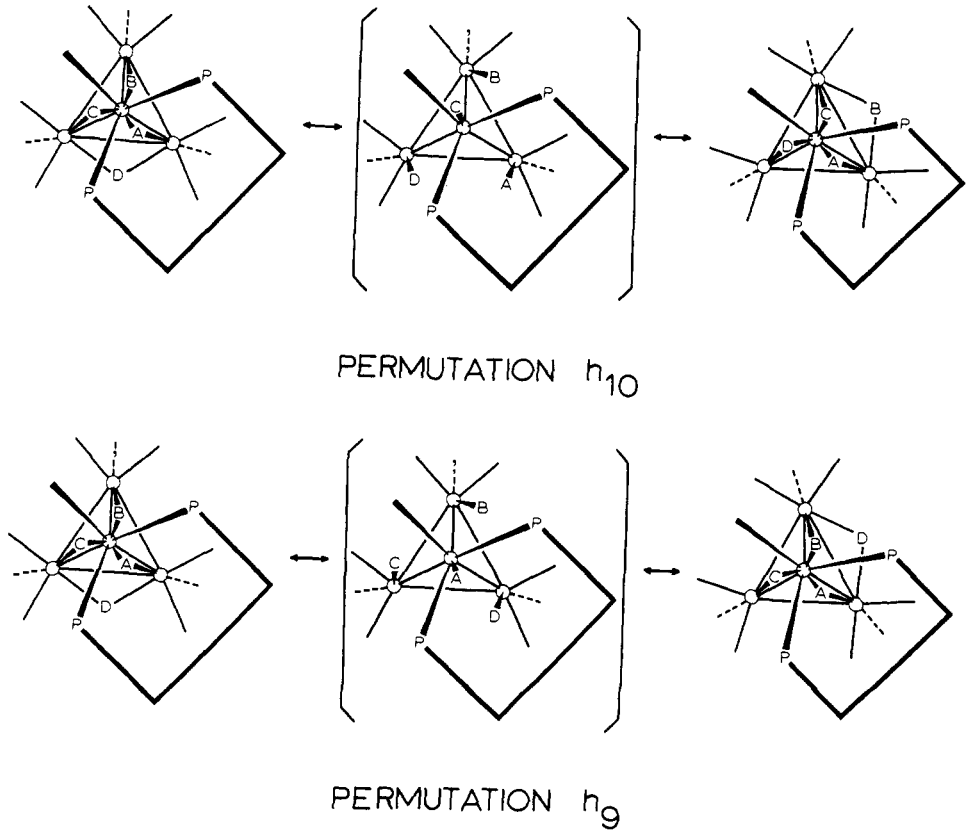

Figure 3. Suggested mechanisms for hydride scrambling in **1** corresponding to permutations h_{10} (upper) and h_9 (lower).

exchange H_C with H_B or H_D, but only interchanges the cis-trans relationships of H_C with respect to the two phosphorus atoms. The lines that remain sharp derive from states in which both phosphorus nuclei have the same spin. Application of the methods of Klemperer[13] lead to a complete set of NMR differentiable permutations (h_2-h_{12})[14] for three-site exchange in a chiral molecule such as **1**. From this set, *only* permutation h_{10} generated computer-simulated spectra[15] that reproduce the differential broadening within the C multiplet (Figure 2, −44 to −31 °C). If resonance C is assigned to the hydride in position H(12) (see Figure 1), a clear mechanistic interpretation of permutation h_{10} is possible,[17] as shown in Figure 3. Movement of H_A to a terminal position on Ru(3) forces H_D to Ru(2), H_C to Ru(1), and H_B to Ru(4). H_A must return to the original edge, but migration of H_B, H_C, and H_D to new edges generates the enantiomeric configuration with the environments of H_B and H_D interchanged. Above −31 °C a second process begins to equilibrate H_C and H_D. The experimental spectra from −25 to 0 °C are accurately simulated (Figure 2) by combining h_{10} with increasing amounts of h_9. At this stage simulations generated from h_9 and h_3 are not distinct, but h_9 has a mechanistic interpretation complementary to that of h_{10} (see Figure 3). In this case H_A moves to Ru(1), H_C to Ru(2), H_B to Ru(4), and H_D to Ru(3). H_A, H_B, and H_C return to their original edges, but H_D migrates to the mirror image position, thereby interchanging H_B and H_C. Activation parameters derived from the spectral fits are $\Delta H^{\ddagger}_{10}$ = 12.8 (0.6) kcal/mol, $\Delta S^{\ddagger}_{10}$ = 2.8 (2.2) gibbs, and $\Delta H^{\ddagger}_9$ = 17.8 (1.0) kcal/mol, $\Delta S^{\ddagger}_9$ = 19.2 (3.8) gibbs.[18]

The edge-terminal-edge pathway provides a consistent picture of the hydride scrambling in **1**,[19] but it is not yet possible to assess the generality of this mechanism for $H_4Ru_4(CO)_{12}$ and other derivatives. The particular arrangement of hydride ligands in **1** may strongly influence the lowest energy exchange mechanism. Alternatively, since in $H_4Re_4(CO)_{12}$ the $M(CO)_3$ moieties are eclipsed with respect to the M-M edges,[3] whereas in **1** they are staggered, the bulky diphosphine ligand may hinder rotation into the eclipsed configuration presumably necessary for a face-bridged intermediate. Nevertheless, these results indicate that terminal hydride intermediates should be considered in experimental and theoretical studies of hydride mobility in H_4M_4 clusters.[20,21]

References and Notes

(1) (a) S. A. R. Knox and H. D. Kaesz, *J. Am. Chem. Soc.*, **93**, 4595 (1971). (b) An x-ray study of $H_4Ru_4(CO)_{12}$ supports the D_{2d} structural assignment (R. Bau, private communication).
(2) R. Saillant, G. Barcelo, and H. D. Kaesz, *J. Am. Chem. Soc.*, **92**, 5729 (1970).
(3) R. D. Wilson and R. Bau, *J. Am. Chem. Soc.*, **98**, 4687 (1976).
(4) G. Huttner and H. Lorenz, *Chem. Ber.*, **108**, 973 (1975).
(5) J. W. Koepke, Ph.D. Thesis, UCLA, 1974.
(6) J. W. Koepke, J. R. Johnson, S. A. R. Knox, and H. D. Kaesz, *J. Am. Chem. Soc.*, **97**, 3947 (1975).
(7) The crystal structure of $H_4W_4(CO)_{12}(OH)_4{\cdot}4OPPhEt_2$ has been determined and terminal positions for the hydride ligands have been proposed.[8] However, the tungsten atoms in this compound are held together by μ_3-hydroxo ligands rather than by direct metal-metal bonds so that it is not a suitable terminal hydride model.
(8) V. G. Albano, G. Ciani, M. Manassero, and M. Sansoni, *J. Organomet. Chem.*, **34**, 353 (1972).
(9) IR (ν_{CO}, $CHCl_3$): 2075 (s), 2046 (vs), 2023 (vs), 2005 (s), 1986 (br m), 1945 (sh) cm^{-1}. Satisfactory elemental analyses have been obtained.
(10) $H_4Ru_4(CO)_{10}Ph_2PCH_2CH_2PPh_2$ crystallizes in the centrosymmetric monoclinic space group $P2_1/c$ with a = 11.89 (1), *b* = 33.565 (40), *c*, 10.269 (1); β = 108.37 (1)°; and *V* = 3885.7 (7) Å^3. The calculated density is 1.858 g cm^{-3} for mol wt 1086.85 and *Z* = 4. Diffraction data were collected on a Syntex $P2_1$ diffractometer, using a wandering ω-scan technique. The structure was solved using a combination of Patterson, difference-Fourier, and full-matrix least-squares refinement techniques, all computations being performed on a Syntex XTL structure-determination system. The final discrepancy indices are R_F 3.8% and R_{wF} 2.5% for the 3630 independent reflections in the range $3° < 2\theta < 40°$ (Mo Kα radiation; *no* reflections rejected).
(11) The two short Ru-Ru distances in $H_4Ru_4(CO)_{10}(PPh_3)_2$ are trans (R. Bau, private communication).
(12) $J(P_1\text{-}H_A) \simeq J(P_2\text{-}H_A)$ = 9 Hz, $J(P_1\text{-}H_C)$ = 30.5 $J(P_2\text{-}H_C)$ = 16 Hz, $J(P_1\text{-}H_B)$ = 18, $J(P_2\text{-}H_B)$ = 28.5 Hz; δ_{P_1} = −70.2, δ_{P_2} = −63.0 ppm (H_3PO_4). Unresolved H-H coupling broadens the individual lines. The fact that the *inner* lines of the C multiplet derive from the ^{31}P $\alpha\alpha$ and $\beta\beta$ states indicates that the two P-H_C coupling constants have opposite signs. The same is probably true for the cis and trans P-H_B coupling constants.
(13) W. G. Klemperer in "Dynamic Nuclear Magnetic Resonance Spectroscopy", F. A. Cotton and L. M. Jackman, Ed., Academic Press, New York, N.Y.,

1975, Chapter 2.
(14) The differentiable permutations are $h_2 = (1)(23)^{vv}$, $h_3 = (12)(3)^{vv}$, $h_4 = (13)(2)^{vv}$, $h_5 = (123)^{vv}$, $h_6 = (132)^{vv}$, $h_7 = (1)(2)(3)^{v^*v}$, $h_8 = (1)(23)^{v^*v}$, $h_9 = (12)(3)^{v^*v}$, $h_{10} = (13)(2)^{v^*v}$, $h_{11} = (123)^{v^*v}$, $h_{12} = (132)^{v^*v}$, where configuration v is determined by (B, C, D) = (1, 2, 3) and v* is the enantiomer of v.
(15) Simulated spectra were calculated with the Whitesides classical multisite exchange computer program EXCHSYS.[16]
(16) G. M. Whitesides and J. S. Fleming, *J. Am. Chem. Soc.*, **89**, 2855 (1967).
(17) If resonance C is assigned to H(14), no mechanistic conclusions follow.
(18) Rate constants determined by visual matching of calculated and experimental spectra were analyzed (weighted least squares, 10 points for h_{10}, 7 points for h_9) by the linearized Eyring equation. Standard deviations in the derived parameters are given in parentheses.
(19) If the assumption that all four hydrogen ligands must move is relaxed, the configurations connected by h_{10} can be interconverted by movements of H_B, H_C, and H_D to adjacent faces, H_A remaining fixed; for h_9 only H_D would move. It is not obvious why these particular partially face-bridged intermediates would be unique; we prefer the more symmetrical all-terminal intermediates.
(20) Extended Hückel calculations (R. Hoffmann, et al., *J. Am. Chem. Soc.*, submitted for publication) on $H_4Fe_4(CO)_{12}$ (carbonyls staggered) indicate relatively little energy difference between face-bridging and edge-bridging (as in either $H_4Ru_4(CO)_{12}$ or **1**) positions for the hydrogen ligands. Terminal positions were not examined.
(21) This work was supported by National Science Foundation Grants CHE 75-14460 (to J.R.S.) and CHE 77-04981 (to M.R.C.). A loan of ruthenium trichloride from Engelhard Industries is gratefully acknowledged.

John R. Shapley,* Steven I. Richter
Department of Chemistry, University of Illinois
Urbana, Illinois 61801

Melvyn Rowen Churchill,* Romana A. Lashewycz
Department of Chemistry
State University of New York at Buffalo
Buffalo, New York 14214
Received July 7, 1977

Single-Crystal Properties of $[Co(C_5H_5NO)_6](NO_3)_2$

Sir:

Several transition metal complexes of pyridine *N*-oxide have been investigated carefully at low temperatures recently, and some remarkably interesting results have been obtained. The series of compounds $M(C_5H_5NO)_6X_2$, with X being either perchlorate or fluoborate, and M^{II} an iron series ion, are rhombohedral and isostructural.[1,2] In the case of the cobalt compounds, magnetic ordering is observed at 0.357 K (BF_4^-) and 0.428 K (ClO_4^-), and the molecules provide the only examples to date of the simple cubic, $S = 1/2$, XY model antiferromagnet.[3-6] The compound $[Ni(C_5H_5NO)_6](ClO_4)_2$ exhibits[7] a very large zero-field splitting of 6.3 K, and the crystal structure and other features of this molecule are such that it provides the first example of a magnetic-field-induced antiferromagnetic phase transition.[8,9] Large zero-field splittings allow the ferrous analogue to be an excellent example of the three-dimensional Ising model,[10] while the copper compounds distort as they are cooled in such a fashion that the perchlorate becomes a one-dimensional antiferromagnet, and the fluoborate provides the best example of the two-dimensional Heisenberg, $S = 1/2$ antiferromagnet.[11]

The great success obtained with the above studies has suggested that it may be profitable to extend these studies by examining the analogous series of nitrates, $[M(C_5H_5NO)_6](NO_3)_2$, and we report here results that in fact appear to confirm this hypothesis. All the salts of the iron series ions have been prepared and found to be isomorphous, but we restrict this report to the cobalt analogue.

Deep-red $[Co(C_5H_5NO)_6](NO_3)_2$ is prepared in the same manner as were the perchlorates[12] and single crystals with satisfactory elemental analysis may be grown from DMF. Using precession camera techniques, we find that the compound belongs to the space group $R\bar{3}$, with $a = 9.487$ Å and $\alpha = 83° 21'$. The measured density is 1.50 g/cm^3, and calculated, for one molecule in this rhombohedral unit cell, is 1.493 g/cm^3. Since the analogous perchlorate compound also belongs[2] to the same space group, with $a = 9.617$ Å, $\alpha = 81.16°$, $Z = 1$, and the fluoborate analogue is isostructural,[1] one may conclude that the three crystals are isomorphous. This observation led us to measure the single-crystal magnetic susceptibilities of the nitrate, in anticipation that they would be similar to those of the perchlorate, and give us guidance on the magnetic ordering behavior to be expected.

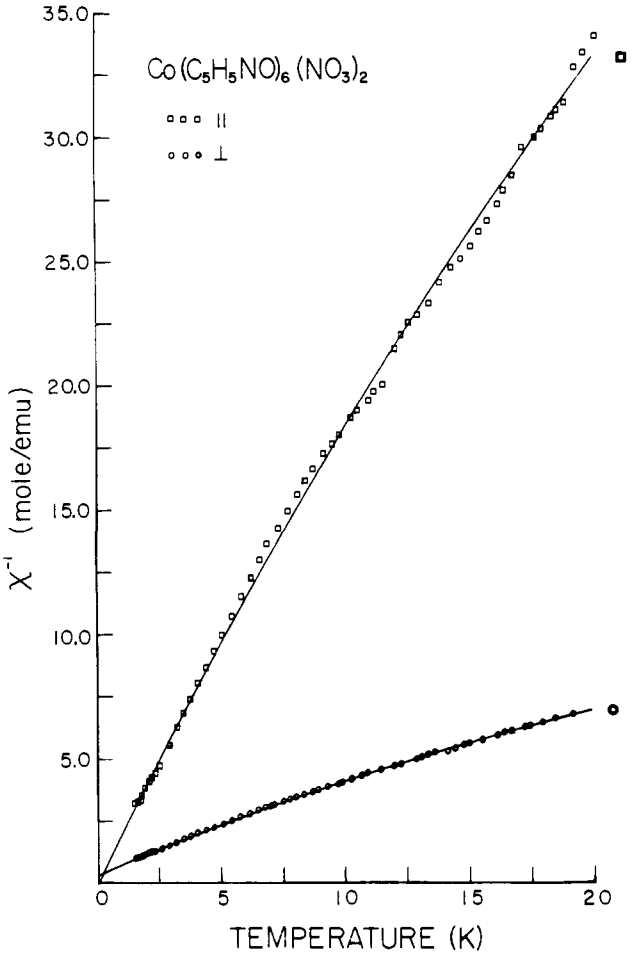

Figure 1. Curie-Weiss plots of the magnetic susceptibilities of $[Co(C_5H_5NO)_6](NO_3)_2$: □, ||; ○, ⊥.

The guide to the discovery of XY magnets lies with the *g*-value anisotropy of the metal atom.[4] In particular, the *g* tensor should have uniaxial symmetry, with $g_\perp \gg g_\parallel$. These conditions were substantially fulfilled by the perchlorate compound, for which susceptibility measurements yielded $g_\parallel = 2.49$ and $g_\perp = 4.70$. The inverse isothermal susceptibilities of $[Co(C_5H_5NO)_6](NO_3)_2$ are plotted as a function of temperature in Figure 1. Normal Curie-Weiss behavior is observed, with the following set of parameters: $g_\parallel = 2.27 \pm 0.05$, $g_\perp = 4.83 \pm 0.05$, $\theta_\parallel = 0.0 \pm 0.05$ K, $\theta_\perp = -0.61 \pm 0.05$ K, TIP(||) = 0.006 emu/mol, and TIP(⊥) = 0.037 emu/mol. The sign of $\theta_\perp$ is antiferromagnetic. These results suggest that $[Co(C_5H_5NO)_6](NO_3)_2$ ought to be as good an example of the XY model magnet as the earlier cases, and probably a better one, since the *g*-value anisotropy is even greater for the nitrate. Furthermore, the crystallographic angle α is slightly larger, tending toward the simple cubic value of 90°. This is important in determining the superexchange path, as well as ensuring that a reference cobalt ion is connected to its six nearest magnetic neighbors by equivalent superexchange paths.

With $\theta_\perp = -0.61$ K, an exchange constant of $J/k = -0.2$